



Synthesis, structural characterization, and antibacterial studies of new borate 13-93B3 bioglasses with low copper dopant

B. M. Elmowafy^{1*}, A.M. Abdelghany², R. M. Ramadan³, R. A. Ghazy¹, T. M. Meaz^{1*}

¹Physics Department, Faculty of Science, Tanta University, Tanta, Egypt

²Spectroscopy Department, Physics Division, National Research Centre, 33 Elbehouth St., Dokki, 12311, Giza, Egypt, ³Microwave Physics and Dielectrics, Physics Division, National Research Centre, 33 Elbehouth St., Dokki, 12311, Giza, Egypt



CrossMark

Abstract

Glasses of nominal composition $(6\text{Na}_2\text{O}.12\text{K}_2\text{O}.5\text{MgO}.20\text{CaO}.4\text{P}_2\text{O}_5.(53-x)\text{B}_2\text{O}_3.x\text{CuO Wt}\%)$ ($0 \leq x \leq 0.6$ wt%) were successfully synthesized via the traditional melt quenching route. The synthesized samples proved to be amorphous without any tendency for crystallization through X-ray diffraction measurements. Structural changes within the glassy matrix and their ability for bone bonding were investigated through employing deconvolution analysis technique (DAT) combined with Fourier transform Infrared (FT-IR) spectral measurement to calculate the percent of tetrahedral boron change versus doping copper ion concentration. It was found that copper additions control the transformation of triangular and tetrahedral coordinated boron that increase with increasing copper content up to 0.4 wt%. UV/Vis. electronic spectral data was used to calculate physical parameters including optical energy gap, refractive index, dielectric permittivity, and other physical parameters. Antimicrobial activity against different pathogenic grams using a cup and disc diffusion method was also correlated to the copper oxide doping level. All previous investigations were used as an optimizing factor for the synthesis of bioactive borate glass suitable for wound healing and wound dressing applications.

Keywords: 13-93B3 Bioglass; Antimicrobial studies; copper oxide; melt quenching; structural characterization.

1. Introduction

Bioactive glass is a class of biomaterials with a specific composition that was recently studied by different authors to treat or replace human tissues both in vitro and in vivo [1-4]. Bioactive glass is first patented by Larry L. Hench in the late 1960s and represents a class of materials that are completely synthetic, compatible, and can bond with the bone. The advancement of materials technology has been immense, particularly in the past 30 years [1]. Bioactive glasses (BGs) usually interact with human fluids that surround tissues creating a strong interfacial bond. Besides, it can control the release of therapeutically active ions over different time intervals which enable bone regeneration and restore the function of the original bone [5, 6]. BGs also, functionalized as a promising material for the controlling of tissue-related disorders including treatment of acute and chronic wounds [7, 8]. Bioactive silicates and borates were recently introduced by different authors with specific compositions to enhance biodegradability and

bioactivity than the first patented 45S5 silicate bioactive glass in bone repair [9-13]. One of the most accentuated differences between traditional silicate and borate bioactive glasses is represented by their relative degradation rates in addition to the faster and safer complete conversion to hydroxyapatite (HA).

Boron is dissolved from borate glass as boric acid $\text{B}(\text{OH})_3$ which is an important component in wound healing [13]. Calcium is necessary for the initiation of epidermal cells and regeneration patterns in the later stages of wound healing and serves as a mineral source for bone growth [14]. As a result, calcium plays an important role in bioactive glasses as a network modifier. Dopant levels of specific ions including but not limited to zinc, copper, and strontium can be assumed as therapeutic agents that enhance osteogenesis and angiogenesis or enzyme cofactor to influence metabolic signaling during the formation of the tissue [15, 16]. Copper also regulates what is called vascular endothelial growth factors (VEGF) and blood vessel formation [17].

*Corresponding author e-mail: belmowafy@yahoo.com

Received date 08 July 2021; revised date 29 December 2021; accepted date 19 January 2022

DOI: 10.21608/EJCHEM.2022.84829.4137

©2022 National Information and Documentation Center (NIDOC)

The human skin can be thought of as the largest organ of the body that serves as a protective barrier against the surrounding environment, a barrier against infection, loss of water, electrolytes, and a thermostat for the body's temperature. Healing of vast areas of full-thickness skin defects is regarded as a major clinical issue [18]. Recent advancements in regenerative medicine and tissue engineering have resulted in a better understanding of wound healing as well as the development of some skin repair and regeneration procedures. Wound dressings made of biomaterials have received a lot of interest in recent years because they can be one of the most straightforward treatments options [19].

On the other hand, bioactive glasses can exert their therapeutic effects in four steps for wound healing, it accelerates the repair of skin and regeneration that is associated with (1) the increased cell proliferation (2) decreased inflammation (3) improve the process of angiogenesis, and (4) the antibacterial effects that result from the presence of bioactive glass in the damaged area [20].

In this study, we used copper oxide as a dopant with a minor addition below 1.0wt% compared with previous studies and the objective of the study is to achieve the desired with low cost and least harmful effect to the human tissue this incorporated with the minor addition of the doped chemical metal and also low toxicity. According to one of the previous studies, Akher Ali [16] stated that CBBGs (CuO derived 1393B3) have better mechanochemical stability than pure 1393B3 borate-based (BBG) in the form of mole% composition, hence glass CBBGs could be used as neo bone tissue regenerative biomaterials. In this present study (13-93B3) borate glass was synthesized, and study the effect of copper oxide on the structure and internal changes using some physical instruments and evaluating their antimicrobial activity besides measuring their physical and FT structural properties.

2. Experimental work

2.1. Materials

Glasses of the composition $(6\text{Na}_2\text{O}.12\text{K}_2\text{O}.5\text{MgO}.20\text{CaO}.4\text{P}_2\text{O}_5.(53-x)\text{B}_2\text{O}_3.x\text{CuO}$ Wt%) ($0 \leq x \leq 0.6$ wt%) as listed in the table (1) were prepared using analytical grade chemical reagent of orthoboric acid as a source for B_2O_3 , Ammonium dihydrogen phosphate as a source of P_2O_5 supplied by Sigma Aldrich Co., while sodium oxide,

potassium oxide, magnesium oxide, and calcium oxide were obtained from their carbonate partner supplied by El Nasr Pharmaceuticals. Whereas Copper oxide was supplied by Riedel De Haen Co. All these chemicals were used as received without further purification. All the weighed batches were mixed and melted in porcelain crucibles in an electrical furnace at about 1100-1150 °C depending on the glass composition. The melts were then quenched and pressed between two steel plates at room temperature to obtain the glass samples.

Table (1) Glass nomination and composition

Glass	Chemical composition (wt.%)						
	Na ₂ O	K ₂ O	MgO	CaO	P ₂ O ₅	B ₂ O ₃	CuO
	6	12	5	20	4	53	0
13-93B3	6	12	5	20	4	52.9	0.1
	6	12	5	20	4	52.8	0.2
	6	12	5	20	4	52.7	0.3
	6	12	5	20	4	52.6	0.4
	6	12	5	20	4	52.4	0.6

2.2 Characterization and testing techniques

Amorphous and glassy nature of the studied samples were tested via XRD machine, XRD PANalytical X'pert pro adopting Cu K α line radiation of wavelength 1.546 Å within the Bragg angles extended between 4 to 70° with a step 0.02°, using a time of 0.4 seconds over a 2 θ diffraction angle range of 4 to 70°. FT-IR spectral data were recorded at room temperature using Nicolet that is 10 a single beam spectrometer within the range 4000-400 cm⁻¹. Spectrum was corrected for background and dark current noises before measurements. The KBr disc route was adopted for measurements using a finely powdered sample mixed with KBr (1:100) in an agate mortar and pressed in the stainless mold with the required dimensions. UV/Vis absorption spectra were measured for polished samples from all synthesized glasses containing variable concentrations of copper oxide dopant within the range extended from 190 to 2500 nm via double beam (JASCO V570 UV/Vis./NIR) double beam spectrophotometer adopting air as a reference sample. The density of bulk samples was measured using Archimedes principle using Xylene (density = 0.865 g/cm³) as an immersion fluid for a triplicate sample from each composition and the average value was recorded at room temperature. Several other physical parameters including polaron radius (r_p), density (ρ),

electronegativity (χ), electron polarizability (α_0), optical basicity (Λ), refractive index (n), and dielectric permittivity (ε) were calculated and interpreted in terms of compositional changes using the following formulas [21-24].

$$r_p = \frac{1}{2} \left(\frac{\pi}{6N} \right)^{\frac{1}{3}} \quad (1)$$

$$\chi = 0.2688 E_g \quad (2)$$

$$\alpha_0 = -0.9 \chi + 3.5 \quad (3)$$

$$\Lambda = -0.5 \chi + 1.7 \quad (4)$$

$$\frac{n^2-1}{n^2+2} = 1 - \left(\frac{E_g}{20} \right)^{1/2} \quad (5)$$

$$\varepsilon = n^2 \quad (6)$$

As 13-93B3 borate glass is used and applied in medical applications so, the antimicrobial test should be done. The antibacterial activity of 13-93B3 borate glass with different dopant levels of copper oxide was examined using the Agar diffusion test adopting both cup and disc techniques. Nutrient agar medium was prepared and inoculated with Gram-positive (*staphylococcus aureus*) and Gram-negative (*Escherichia coli*) bacteria as well as fungi (*Candida albicans* and *Aspergillus niger*) [24]. Bacteria and fungi were incubated and spread out homogeneously on a Petri dish and the glass pellets made from powder were used in the case of the disc method. On the other hand for the cup method agar solution was prepared and poured on a petri dish then we incubate microbial inoculum on the entire agar surface and the media plate is perforated and then added the samples. The inhibition zone was recorded for each sample for a three-replicated sample of each composition after 24 h.

3. Results and Discussion

3.1. XRD analysis

X-ray diffraction (XRD) was used to examine the crystalline or amorphous nature or formed phases within the tested powdered samples of the synthesized 13-93B3 borate glass doped with different copper oxide contents. The XRD shown in figure (1) displayed an amorphous structure in the series and no evidence of crystalline phase. After the addition of copper oxide, a broadening of the broad hump at 2θ of about 30° was observed with no observed distinct or incessant sharp peaks that characterizing amorphous glassy structure.

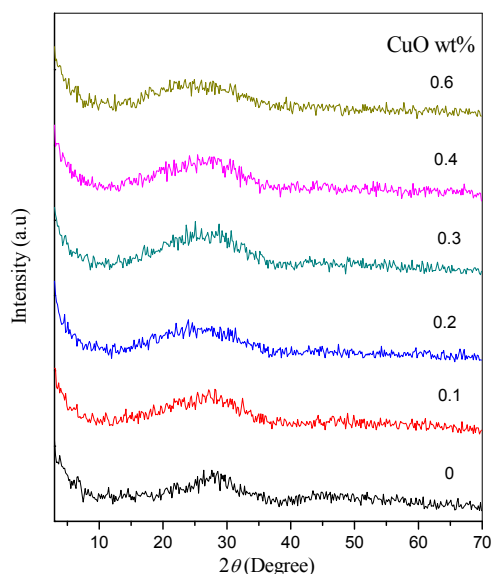


Figure (1) X-ray diffraction pattern of synthesized glasses containing different copper oxide concentrations

3.2. Fourier Transform Infrared Analysis (FTIR)

The analysis of 13-93B3 borate glass with CuO addition was studied using FTIR spectroscopic technique. FTIR spectra identify structural groups of the matrix even if they are amorphous or crystalline glass and the compositional changes in the glass matrix after adding the dopant. FTIR was measured for the based glass and doped glasses which contain a different concentration of copper oxide Figure (2). The main vibrational groups observed within the wavenumber range-extended between $1350-1450 \text{ cm}^{-1}$ and at $690-720 \text{ cm}^{-1}$ assigned to the B-O stretching and bending modes of trivalent BO_3 groups. Vibrational bands within the region $900-1100 \text{ cm}^{-1}$ assigned to the B-O stretching mode of BO_4 groups as previously reported and analyzed by different authors [11, 13, 25].

3.3. Deconvolution Analysis Technique (DAT)

Structural analysis of the functional building groups of borate glass can be tested using traditional DAT that is used as a quantitative tool for the determination of the fraction of four coordinated borons ($N_4 = \text{BO}_4/(\text{BO}_4+\text{BO}_3)$). The spectral data within the range from $500-1750 \text{ cm}^{-1}$ that contain the principle vibrational modes of borate building units were considered.

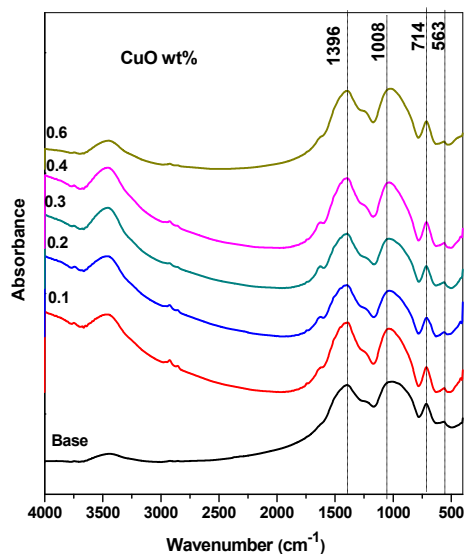
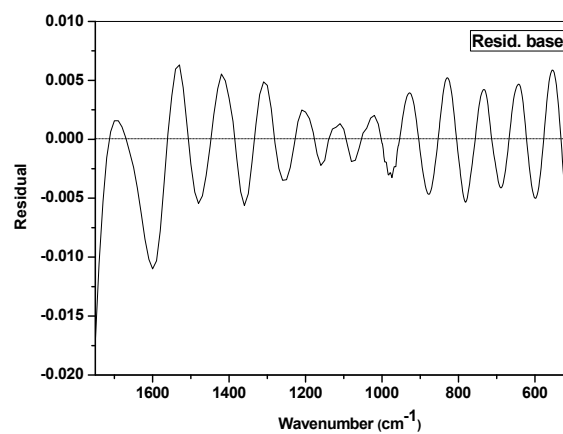
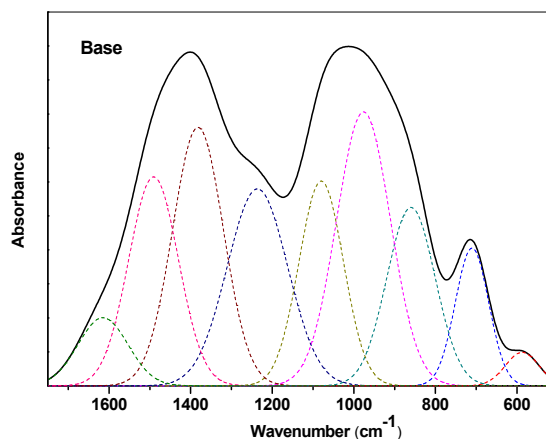


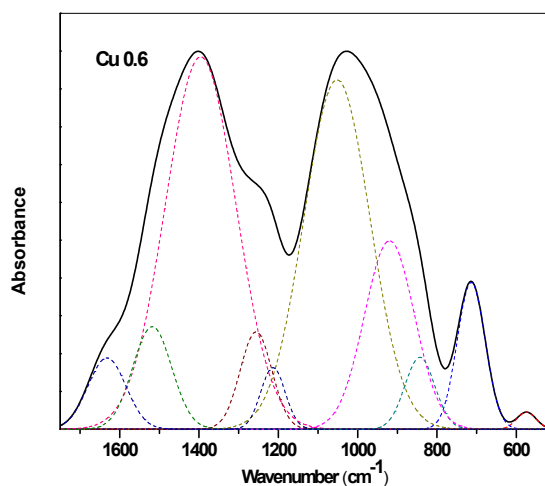
Figure (2) FT-IR optical absorption spectra of synthesized glasses containing different copper oxide concentrations

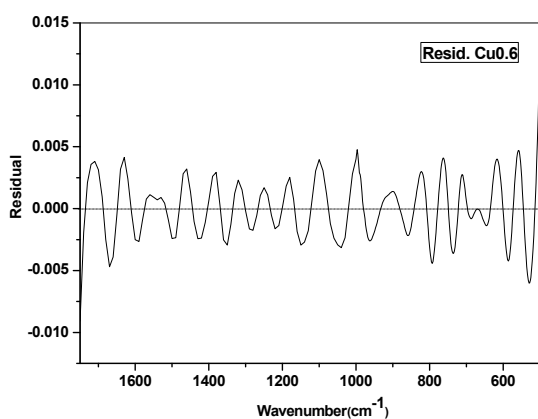
An exemplified analysis curve is shown in Figure (3). The remind region contains only the vibrational mode of the OH group within the range extended from 3600-3200 cm^{-1} . Quantitative analysis for the infrared spectrum has been analyzed and stimulated by Gaussian functions using the standard curve fitting [Peak Fit] program in which peak positions of each band intensities and widths have been varied automatically by the program to find the best fit. The program was designed to define hidden peaks using numerical alternative methods and suitable peak definition including height, intensity, and full width at half maximum (FWHM) and other remind factors that control the quality of the fitting process. The spectra of IR were corrected for the noises of the dark current and background using a two-point baseline correction before fitting. Many trials have been applied using the multi-band of components based on minimization of the deviations between the simulated and experimental spectrum [26, 27] to resolve all smearing overlapped bands attributed for both triangular and tetrahedral borate groups. The variations of N4 were calculated and plotted against copper concentration as shown in Figure (4). Figure (4) the addition of Copper oxide content to the borate glass matrix makes a differing effect in the network of the borate glass, of tetrahedrally coordinated boron (triangular and tetrahedral coordinate). This differing effect increased until reaches the concentration (0.2)

of copper content this is the point of transformation and then decreased rapidly.



(a)





(b)

Figure (3a, b) DAT with residuals for FT-IR spectral data of some selected samples.

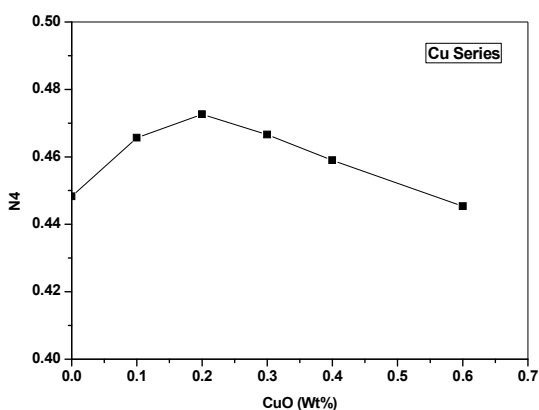


Figure (4) Variation of the fraction of four coordinated boron versus copper content.

3.4. UV/Vis./NIR electronic Spectra

Figure (5) shows UV/Vis./NIR optical absorption spectra of polished base 13-93B3 glass with other samples of the same composition containing different amounts of dopant copper oxide within the wavelength range between 200-2500 nm.

The base glass shows a sharp intense band within the UV region originally located at 250 nm previously reported by different glass scientists [13, 24] and attributed for the presence of iron oxide as impurity traces even in ppm level in the chemicals or refractories during the preparation process and without any further bands till the end of measurements. Copper-doped glasses show the appearance of an additional visible band centered at

about 745 nm with different intensities based on the copper content. The variation of the absorption intensity of this band was correlated with copper content as shown in Figure (6).

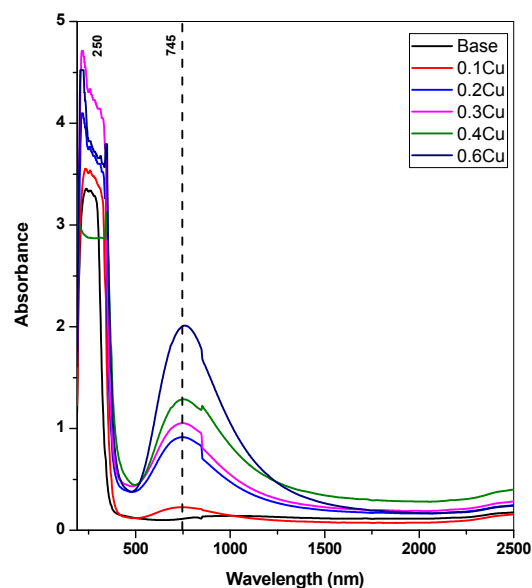


Figure (5) UV/Vis./NIR optical absorption spectra of studied samples

3.5. Calculated physical parameters

Optical energy gap (E_g) both for direct and indirect transitions obtained from Tauc's plot of photon energy ($h\nu$) versus both $(\alpha h\nu)^{1/2}$ and $(\alpha h\nu)^2$ respectively are shown for selected samples in Figure (7) and tabulated in Table (2). Besides, other physical parameters including polaron radius (r_p), density (ρ), electronegativity (χ), electron polarizability (α_0), optical basicity (Λ), refractive index (n), and dielectric permittivity (ϵ) calculated using Dimitrov and Sakaa equation [22, 24] were calculated and listed in Table (2).

Obtained data reveal a strong correlation between physical characteristics and copper oxide content within the glassy matrix even in such dopant level as revealed from four coordinated boron (Figure (4)), the optical density at 745 nm (Figure (5)), and the estimated density (Figure (8)). All measurements support the boundary concentration that affects these characteristics to about 0.2 wt% Copper oxide with observable changes. Such a finding may be attributed to the nature of the dopant or nominal composition of the matrix.

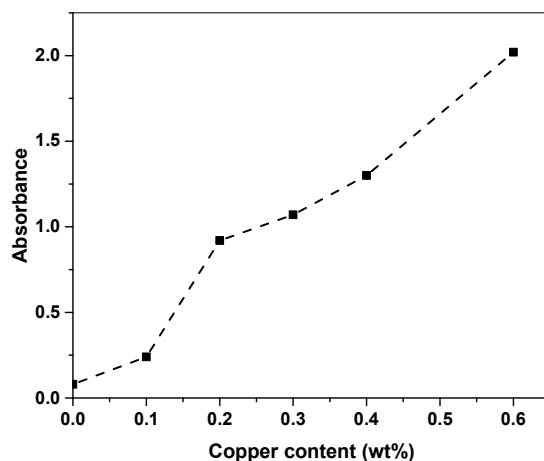


Figure (6) variation of the absorption intensity at 745 nm with copper oxide content

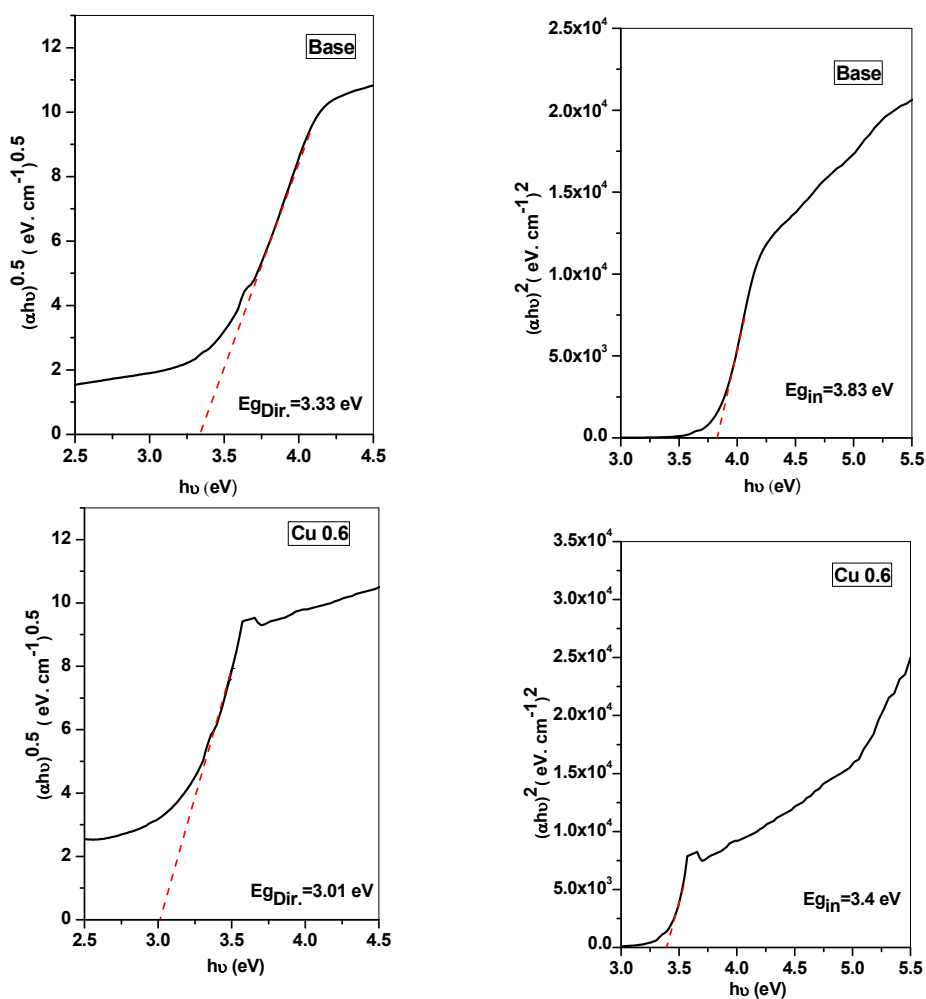


Figure (7) Optical energy gap (E_g) both for direct and indirect transitions obtained from Tauc's plot of photon energy ($h\nu$) versus both $(\alpha h\nu)^{1/2}$ and $(\alpha h\nu)^2$

Sample	E_{opt}	E_{di} (eV)	E_{ind}	r_p (m)	ρ (g/cm ³)	χ	α_0 (eV)	Λ	N	ϵ
Base	3.48±0.08	3.33	3.83	-	2.617	0.888	2.701	1.256	2.312	5.345
0.1Cu	3.26±0.06	3.17	3.54	1.31×10^{-11}	2.627	0.846	2.739	1.277	2.353	5.537
0.2Cu	3.14±0.05	3.05	3.52	9.30×10^{-12}	2.635	0.814	2.768	1.293	2.383	5.579
0.3Cu	3.07±0.06	3.03	3.52	7.59×10^{-12}	2.637	0.808	2.772	1.296	2.389	5.707
0.4Cu	2.91±0.04	2.83	3.34	6.57×10^{-12}	2.632	0.755	2.820	1.322	2.441	5.958
0.6Cu	3.07±0.06	3.01	3.40	5.37×10^{-12}	2.629	0.803	2.777	1.298	2.395	5.736
±SD	0.196	0.168	0.169	3.65×10^{-11}	0.007	0.045	0.040	0.022	0.043	0.208
±SE	0.033	0.028	0.028	6.07×10^{-12}	0.001	0.007	0.007	0.004	0.007	0.035

Table (2) Optical Energy gap and other calculated physical parameter

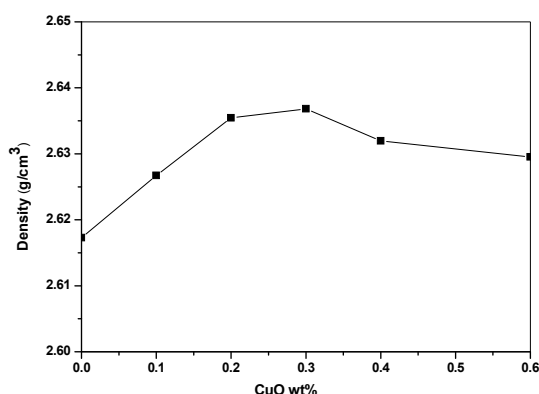


Figure (8) variation of the bulk density of synthesized samples with copper oxide content

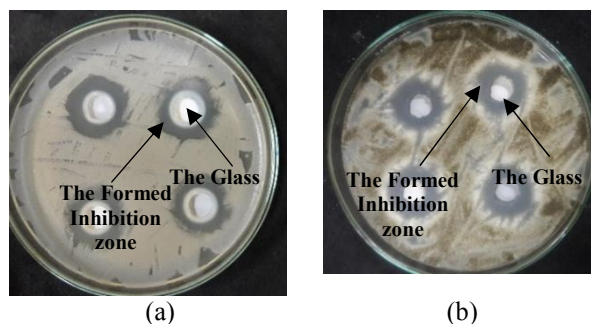
3.6. Antibacterial Activity

The antimicrobial activity is estimated by testing microorganisms against the BGs samples. Pulverized powders of the studied glasses were added separately to the culture medium and incubated for 24h [28]. Exemplified inhibition zones are formed and estimated as shown in figure (9). The activity index (%) [27, 29, 30] resulted from both agar disc and cup diffusion against test bacteria and fungi were calculated according to the following formula as the based glass without doping considered as standard which is shown in Figure (10) and presented in both tables (3 and 4) below.

% Activity Index

$$= \frac{\text{Zone of inhibition by test compound (diameter)}}{\text{Zone of inhibition by standard (diameter)}} \times 100 \quad (7)$$

From the data in the tables, it was noticed that 13-93B3 borate glasses doped with minor copper contents showed an observed antibacterial effect associated with the gram-positive bacteria *Staphylococcus aureus* (*S. aureus*) in the case of cup method especially for samples Cu0.2 and Cu0.3

Figure (9) Exemplified inhibition zones of different 13-93B3 glasses doped with copper oxide against (a) Gram-positive (*staphylococcus aureus*), (b) Fungus (*Aspergillus niger*)

concentrations. On the other hand, Cu0.2 and Cu0.4 were efficient to inhibit the growth of gram-negative bacteria *Escherichia coli* (*E. coli*) in the case of the Disc method. Besides, sample Cu0.2 showed a significant antibacterial and antifungal effect versus activity index for bacteria and fungi for two methods. It was concluded that Cu minor addition to the borate Bioglass 13-93B3 provides a good inhibition for gram-positive, gram-negative bacteria, and fungi in different methods attributed for the presence of copper in different oxidation states within the glassy matrix.

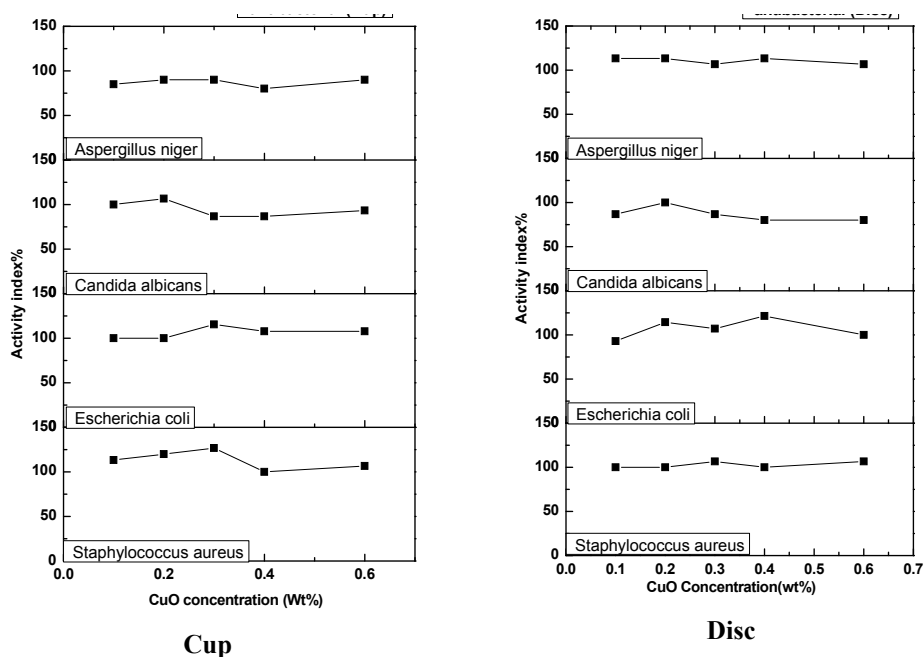


Figure (10) Activity index versus concentration of studied glasses using (a) Cup, (b) Disc method.

Glass	<i>S. aureus</i>		<i>E. coli</i>		<i>C. albicans</i>		<i>A. niger</i>	
	<i>D (mm)</i>	<i>A%</i>	<i>D (mm)</i>	<i>A%</i>	<i>D (mm)</i>	<i>A%</i>	<i>D (mm)</i>	<i>A%</i>
Cu0.1	17	113.33	13	100.00	15	100.00	17	85
Cu0.2	18	120.00	13	100.00	16	106.67	18	90
Cu0.3	19	126.67	15	115.38	13	86.67	18	90
Cu0.4	15	100.00	14	107.69	13	86.67	16	80
Cu0.6	16	106.67	14	107.69	14	93.33	18	90
Base	15	100	13	100	15	100	20	100

Table (3) Diameter of inhibition zone (*D*) and the calculated activity index (*A*) using cup method in comparison to the base glass.

Glass	<i>S. aureus</i>		<i>E. coli</i>		<i>C. Albicans</i>		<i>A. niger</i>	
	<i>D (mm)</i>	<i>A%</i>	<i>D (mm)</i>	<i>A%</i>	<i>D (mm)</i>	<i>A%</i>	<i>D(mm)</i>	<i>A%</i>
Cu0.1	15	100.00	13	92.86	13	86.67	17	113.33
Cu0.2	15	100.00	16	114.29	15	100.00	17	113.33
Cu0.3	16	106.67	15	107.14	13	86.67	16	106.67
Cu0.4	15	100.00	17	121.43	12	80.00	17	113.33
Cu0.6	16	106.67	14	100.00	12	80.00	16	106.67
Base	15	100	14	100	15	100	15	100

Table (4) Diameter of inhibition zone (*D*) and the calculated activity index (*A*) using Disc method in comparison to the base glass.

All tested samples showed clear inhibition zones and activity index against bacterial and fungi. So borate bioactive glass is a good material to be used in medical application due to its antimicrobial effect

which can reduce infection by inhibiting bacterial growth or killing bacteria so, it was also noticed that the Inhibition zone and activity index were found to increase with the doping process against different pathogenic grams using cup and disc diffusion

method regardless of the doping level. All previous data suggested the suitability of the studied glasses (13-93B3 borate glass) doped with copper oxide to innervate the antimicrobial activity in wound healing.

So, copper is one of the most widely used therapeutic metals in biomedicine with applications ranging from antibacterial to cancer theranostics. This element may be easily incorporated into a variety of biomaterials; in particular, copper-doped bioactive glasses (BGs) give opportunities for biomedical engineers and physicians as regards their excellent biocompatibility and regenerative potential [31].

4. Conclusion

Base 13-93B3 patented glass and other samples containing up to 0.6 wt% copper oxide were successfully synthesized via the traditional melt quenching route. The amorphous structure of synthesized samples was approved using the XRD route. Effects of copper oxide doping were investigated through conversion of structural building groups using deconvolution analysis technique (DAT) adopted for the calculation of N₄ fraction. The number of tetrahedrally coordinated boron was found to increase with increasing copper content up to 0.4 wt%. UV/Vis/NIR spectral data reveal the appearance of an extra band in the visible region at about 745nm whose intensity was found to be sensitive to the doping level of copper oxide. Changes in different physical parameters show a boundary condition at nearly 0.2wt% of copper oxide which represents an optimizing concentration of dopant that led to an extreme density, N₄, and other calculated parameters. Inhibition zone and activity index were found to increase with the doping process against different pathogenic grams using the cup and disc diffusion method. All previous investigations were used as an optimizing factor for the synthesis of bioactive borate glass with the minor addition of copper oxide to achieve the desired purpose to be suitable for wound healing application.

5. References

- [1] Hench, L. L. The story of Bioglass®. *Journal of Materials Science: Materials in Medicine*, 17(11), (2006), 967-978.
- [2] Gerhardt, L. C., & Boccaccini, A. R. Bioactive glass and glass-ceramic scaffolds for bone tissue engineering. *Materials*, 3(7), (2010), 3867-3910.
- [3] Mutlu, N., Kankova, H., Galuskova, D., Galusek, D., & Boccaccini, A. R. Incorporation of Zinc Doped Borate Bioactive Glasses into Soft Matrices for Wound Healing Applications. *FunGlass School, part1* (2019), May 20-22.
- [4] Cui, X., Zhang, Y., Wang, H., Gu, Y., Li, L., Zhou, J., ... & Rahaman, M. N. An injectable borate bioactive glass cement for bone repair: preparation, bioactivity and setting mechanism. *Journal of Non-Crystalline Solids*, 432, (2016), 150-157.
- [5] Kokubo, T., & Takadama, H., How useful is SBF in predicting in vivo bone bioactivity?. *Biomaterials*, 27(15), (2006), 2907-2915.
- [6] Takadama, H., Kim, H. M., Kokubo, T., & Nakamura, T., TEM-EDX study of mechanism of bonelike apatite formation on bioactive titanium metal in simulated body fluid. *Journal of Biomedical Materials Research: An Official Journal of The Society for Biomaterials, The Japanese Society for Biomaterials, and The Australian Society for Biomaterials and the Korean Society for Biomaterials*, 57(3), (2001),441-448.
- [7] Gruian, C., Vanea, E., Simon, S., & Simon, V., FTIR and XPS studies of protein adsorption onto functionalized bioactive glass. *Biochimica et Biophysica Acta (BBA)-Proteins and Proteomics*, 1824(7), (2012), 873-881.
- [8] Mârza, S. M., Magyari, K., Bogdan, S., Moldovan, M., Peştean, C., Nagy, A., ... & Papuc, I., Skin wound regeneration with bioactive glass-gold nanoparticles ointment. *Biomedical Materials*, 14(2), (2019), 025011.
- [9] Huang, W., Day, D. E., Kittiratanapiboon, K., & Rahaman, M. N., Kinetics and mechanisms of the conversion of silicate (45S5), borate, and borosilicate glasses to hydroxyapatite in dilute phosphate solutions. *Journal of Materials Science: Materials in Medicine*, 17(7), (2006), 583-596.
- [10] Fu, Q., Rahaman, M. N., Bal, B. S., Brown, R. F., & Day, D. E., Mechanical and in vitro performance of 13–93 bioactive glass scaffolds prepared by a polymer foam replication technique. *Acta biomaterialia*, 4(6), (2008), 1854-1864.
- [11] Liang, W., Rahaman, M. N., Day, D. E., Marion, N. W., Riley, G. C., & Mao, J. J. Bioactive borate glass scaffold for bone tissue engineering. *Journal of Non-Crystalline Solids*, 354(15-16), (2008), 1690-1696.
- [12] Rahaman, M. N., Day, D. E., Bal, B. S., Fu, Q., Jung, S. B., Bonewald, L. F., & Tomsia, A. P., Bioactive glass in tissue engineering. *Acta biomaterialia*, 7(6), (2011), 2355-2373.
- [13] Okasha, A., Abdelghany, A. M., Wassel, A. R., & Menazea, A. A., Bone bonding augmentation and synergetic attitude of gamma-irradiated modified borate bioglass. *Radiation Physics and Chemistry*, 176, (2020), 109018.

- [14] Li, T., Yan, A., Bhatia, N., Altinok, A., Afik, E., Durand-Smet, P., ... & Meyerowitz, E. M., Calcium signals are necessary to establish auxin transporter polarity in a plant stem cell niche. *Nature communications*, 10(1), (2019), 1-9.
- [15] El-Dafrawy, S. M., Farag, M., & Hassan, S. M., Photodegradation of organic compounds using chromium oxide-doped nano-sulfated zirconia. *Research on Chemical Intermediates*, 43(11), (2017), 6343-6365.
- [16] Ali, A., Singh, B. N., Yadav, S., Ershad, M., Singh, S. K., Mallick, S. P., & Pyare, R. CuO assisted borate 1393B3 glass scaffold with enhanced mechanical performance and cytocompatibility: An In vitro study. *Journal of the Mechanical Behavior of Biomedical Materials*, 114, (2021), 104231.
- [17] Hu, K., & Olsen, B. R., The roles of vascular endothelial growth factor in bone repair and regeneration. *Bone*, 91, (2016), 30-38.
- [18] Lee, S. H., Jeong, S. K., & Ahn, S. K., An update of the defensive barrier function of skin. *Yonsei medical journal*, 47(3), (2006), 293.
- [19] Pina, S., Oliveira, J. M., & Reis, R. L., Natural□based nanocomposites for bone tissue engineering and regenerative medicine: A review. *Advanced Materials*, 27(7), (2015), 1143-1169.
- [20] Kargozar, S., Hamzehlou, S., & Baino, F., Can bioactive glasses be useful to accelerate the healing of epithelial tissues?. *Materials Science and Engineering: C*, 97, (2019), 1009-1020.
- [21] Duffy, J. A., A review of optical basicity and its applications to oxidic systems. *Geochimica et Cosmochimica Acta*, 57(16), (1993), 3961-3970.
- [22] Dimitrov, V., & Sakka, S., Electronic oxide polarizability and optical basicity of simple oxides. I. *Journal of Applied Physics*, 79(3), (1996), 1736-1740.
- [23] Dimitrov, V., & Komatsu, T., Electronic polarizability, optical basicity and non-linear optical properties of oxide glasses. *Journal of non-crystalline solids*, 249(2-3), (1999), 160-179.
- [24] Abdelghany, A. M., & Behairy, A., Optical parameters, antibacterial characteristics and structure correlation of copper ions in cadmium borate glasses. *Journal of Materials Research and Technology*, 9(5), (2020), 10491-10497.
- [25] Abdelghany, A. M., ElBatal, H. A., & EzzElDin, F. M., Bone bonding ability behavior of some ternary borate glasses by immersion in sodium phosphate solution. *Ceramics International*, 38(2), (2012), 1105-1113.
- [26] Kamitsos, E. I., Infrared studies of borate glasses. *Physics and Chemistry of Glasses*, 44(2), (2003), 79-87.
- [27] Abdelghany, A. M., The elusory role of low level doping transition metals in lead silicate glasses. *Silicon*, 2(3), (2010), 179-184.
- [28] Yuan, J. J., Yan, H. J., He, J., & Liu, Y. Y. Antibacterial activities of polyphenols from olive leaves against *Klebsiella pneumoniae*. In *IOP Conference Series: Earth and Environmental Science*, 680(1), (2021), 012060.
- [29] Namazi, H., Polymers in our daily life, *BioImpacts*, 7 (2017), 73-74.
- [30] Du Prez, F., Hoogenboom, R., Klumperman, B., Meier, M., Monteiro, M., Müller, A., & Vancso, G. J., Fifty years of polymer science. *European polymer journal*, 65, (2015), 3.
- [31] Kargozar, S., Mozafari, M., Ghodrati, S., Fiume, E., Baino, F., Copper-containing bioactive glasses and glass-ceramics: From tissue regeneration to cancer therapeutic strategies. *Materials Science and Engineering: C*, 121, (2021), 111741.